

# Natural history of atherosclerotic disease progression as assessed by $^{18}\text{F}$ -FDG PET/CT

Holger Hetterich<sup>1</sup> · Axel Rominger<sup>2</sup> · Lisa Walter<sup>1</sup> · Maximilian Habs<sup>3</sup> · Sarah Volpers<sup>2</sup> · Marcus Hacker<sup>4</sup> · Maximilian F. Reiser<sup>1</sup> · Peter Bartenstein<sup>3</sup> · Tobias Saam<sup>1</sup>

Received: 10 January 2015 / Accepted: 13 April 2015 / Published online: 22 April 2015  
© Springer Science+Business Media Dordrecht 2015

**Abstract** The aim of this study was to assess the impact of cardiovascular risk factors and plaque inflammation on the progression of atherosclerosis as assessed by positron emission tomography/computed tomography (PET/CT) imaging with  $^{18}\text{F}$ -radiolabelled fluorodeoxyglucose ( $^{18}\text{F}$ -FDG). This study was designed as a retrospective cohort study. Patients who received a  $^{18}\text{F}$ -FDG PET/CT scan and follow-up scan 9–24 months later without systemic inflammation or steroid medication were eligible for the study.  $^{18}\text{F}$ -FDG PET/CT included a full diagnostic contrast enhanced CT scan. Cardiovascular risk factors and medication were documented. Calcified plaque volume, lumen area and  $^{18}\text{F}$ -FDG uptake, quantified by the target-to-background ratio (TBR), were measured in the carotid arteries, aorta and iliac arteries. Influence of cardiovascular risk factors and vessel wall inflammation on atherosclerotic disease

progression was analyzed. Ninety-four patients underwent baseline and follow-up whole body  $^{18}\text{F}$ -FDG PET/CT (mean follow-up time  $14.5 \pm 3.5$  months). Annualized calcified plaque volume increased by 15.4 % ( $p < 0.0001$ ), carotid and aortic lumen area decreased by 10.5 % ( $p < 0.0001$ ) and 1.7 % ( $p = 0.045$ ). There was no significant difference in  $^{18}\text{F}$ -FDG uptake at baseline and follow-up (mean TBR  $1.44 \pm 0.18$  vs.  $1.42 \pm 0.19$ ,  $p = 0.18$ ). Multiple linear regression analysis identified hypertension as an independent predictor for total, aortic and iliac calcified plaque volume progression (all  $p < 0.04$ ). Carotid lumen reduction was predicted by hypercholesterolemia ( $p = 0.008$ ) while aortic lumen reduction was associated with BMI and mean  $^{18}\text{F}$ -FDG uptake ( $p \leq 0.005$ ). Furthermore we observed a dose response relationship between the number of cardiovascular risk factors and calcified plaque volume progression in the aorta ( $p = 0.03$ ). Findings from this study provide data on the natural history of atherosclerotic disease burden in multiple vascular beds and emphasize the value of morphological and physiologic information provided by  $^{18}\text{F}$ -FDG PET/CT imaging.

Holger Hetterich and Axel Rominger have contributed equally to this work.

**Electronic supplementary material** The online version of this article (doi:10.1007/s10554-015-0660-8) contains supplementary material, which is available to authorized users.

✉ Holger Hetterich  
Holger.Hetterich@med.uni-muenchen.de

- <sup>1</sup> Institute of Clinical Radiology, Ludwig-Maximilians-University Hospital, Marchioninistr. 15, 81377 Munich, Germany
- <sup>2</sup> Department of Nuclear Medicine, Ludwig-Maximilians-University Hospital, Munich, Germany
- <sup>3</sup> Department of Neurology, Ludwig-Maximilians-University Hospital, Munich, Germany
- <sup>4</sup> Division of Nuclear Medicine, Department of Biomedical Imaging and Image-guided Therapy, Medical University of Vienna, Vienna, Austria

**Keywords** Atherosclerosis · Plaque imaging · FDG · PET/CT · Cardiovascular risk factors

## Introduction

Atherosclerosis is a systemic vascular disease characterized by intimal plaque formation [1]. Plaque rupture or erosion can lead to thromboembolic events such as myocardial infarction and stroke, which are an important cause of morbidity and mortality in both developing and

industrialized countries [2, 3]. Non-invasive imaging of atherosclerosis has become increasingly popular as it has been shown that several markers, such as intima media thickness measurements by ultrasound [4], identification of carotid plaque hemorrhage by magnetic resonance imaging [5] as well as assessment of coronary calcified plaque burden [6], luminal stenosis [7] and increased pericardial fat volume [8] by computed tomography (CT) are associated with cerebro- or cardiovascular events. However most of these imaging modalities are limited as they provide primarily morphological information of one vascular bed and physiological information is not available. Positron emission tomography/computed tomography (PET/CT) imaging with  $^{18}\text{F}$ -radiolabeled fluorodeoxyglucose ( $^{18}\text{F}$ -FDG) is able to derive physiological and morphological information of various vascular beds non-invasively and it has previously been shown by our group that  $^{18}\text{F}$ -FDG uptake is a strong predictor of future cardio- or cerebrovascular events in cancer patients [9].

Therefore  $^{18}\text{F}$ -FDG PET/CT has become increasingly popular to study the physiology of the atherosclerotic disease process [9–12] and several studies are under way which use PET/CT prospectively to identify PET/CT derived markers which might help to identify patients at risk for subsequent events [13]. Interestingly, to date little data exists that describes the natural progression of functional and morphological variables of atherosclerosis as derived by  $^{18}\text{F}$ -FDG PET/CT as well as potentially influencing factors.

The aims of this study were (1) to assess the natural history of calcified plaque burden, vascular luminal area and  $^{18}\text{F}$ -FDG-uptake and (2) to assess the impact of cardiovascular risk factors and plaque inflammation on atherosclerotic disease progression or regression.

## Materials and methods

### Patient selection and follow-up

This study was designed as a retrospective cohort study. Institutional review board (IRB) approval was waived given the retrospective study design. Patients of at least 40 years of age who were referred to our institution for a diagnostic, contrast enhanced  $^{18}\text{F}$ -FDG PET/CT scan between 2011 and 2012 and a follow-up contrast enhanced  $^{18}\text{F}$ -FDG PET/CT scan 9–24 months later were eligible for the study. Patients with prior or ongoing steroid medication, inflammation of unknown origin, sepsis, vasculitis or ongoing radiation were excluded from the study. Cardiovascular risk factors as well as relevant medications and other important clinical information were recorded during the first  $^{18}\text{F}$ -FDG PET/CT scan in our institution by chart review. Hypertension was defined as a repeatedly elevated systolic pressure of  $\geq 140$  mmHg or

a diastolic pressure of  $\geq 90$  mmHg. Diabetes was defined as a fasting plasma glucose level of  $\geq 126$  mg/dL or a plasma glucose level in a 2 h oral glucose tolerance test of  $\geq 200$  mg/dL. Hypercholesterolemia was defined as LDL levels  $>160$  mg/dL or total cholesterol levels above 240 mg/dL. Body mass index was defined as the body mass divided by the square of the height. A positive family history is defined as a parent and/or sibling with a history of treated angina, myocardial infarction, percutaneous coronary catheter interventional procedure, coronary artery bypass grafting, stroke or sudden cardiac death before 55 years in men or 65 years in women. Coronary artery disease was defined as stenosis of more than 50 % in coronary angiography, status post revascularization, myocardial infarction or unstable angina. A cardiac event was defined as myocardial infarction or unstable angina. A cerebrovascular event was defined as ischemic stroke, transient ischemic attack or amaurosis fugax.

### Imaging technique

All  $^{18}\text{F}$ -FDG PET/CT examinations were performed on a Gemini PET/CT scanner (Philips Healthcare, Hamburg, Germany). The system consists of a germanium oxyorthosilicate fullring PET scanner and a 2-detector-row CT scanner. Patients fasted for at least 6 h before the scan to ensure a serum glucose level below 130 mg/dL. Before the scan 20 mg of furosemide, 20 mg of butylscopolamine bromide and 5 MBq/kg of body weight  $^{18}\text{F}$ -FDG (mean dose 240 MBq, range 200–480 MBq) were administered intravenously. Afterwards patients rested for 45 min. Transmission data was acquired 60 min after injection of  $^{18}\text{F}$ -FDG by means of a diagnostic contrast enhanced (Ultravist 370, Bayer-Schering AG, Berlin, Germany) venous phase CT-scan extending from the base of the skull to the proximal thighs using the following parameters: tube current 195 mAs, tube potential 120 kV, matrix  $512 \times 512$ , slice thickness 6 mm, increment 5 mm/s, rotation time 0.5 s, pitch factor 1.5. The CT-scan was performed during breath hold. After CT examination PET data were acquired in 3-dimensional mode with a  $144 \times 144$  matrix. The emission scan duration per bed position was 2.5 min. Following scatter and decay correction PET data were reconstructed iteratively with and without attenuation correction and axial, coronal and sagittal reformats were produced.

### Image analysis

All  $^{18}\text{F}$ -FDG PET/CT data were read by a board certified nuclear medicine physician and board certified radiologist with more than 10 years experience in vascular imaging in consensus decision, who were blinded to all clinical patient data and to the time point of the examination. Maximal standardized uptake values (SUV) for  $^{18}\text{F}$ -FDG were

measured in three cross-sections of each of the following main arterial segments: both common carotid arteries, thoracic aorta, abdominal aorta and both iliac arteries. To measure SUV, circular regions of interest (ROIs) were placed over the carotid and iliac vessels to fully cover the arterial wall. In larger vessels, ROIs with a diameter of 1 cm were slid along the circumference of the arterial wall to locate and measure the maximal SUV of the segment. Measurements were performed over the whole vessel axis. All measurements were performed on axial  $^{18}\text{F}$ -FDG PET/CT images as previously described [9, 14].

For blood-pool SUV measurements, three 1-cm-diameter ROIs were placed in the mid lumen of the inferior vena cava, the superior vena cava, and the right atrium. Mean blood-pool activity was calculated from these measurements. Measurements are illustrated in Fig. 1.

Target-to-background ratio (TBR) was calculated for each arterial segment as the ratio of maximal SUV in the segment and blood-pool SUV. Mean TBR values were calculated for carotid arteries, thoracic aorta, abdominal aorta, aorta and iliac arteries as well as all segments combined.

Lumen area measurements were performed manually on axial CT images with fixed window settings optimized for vascular CT. Mean aortic lumen area was measured at 20 consecutive locations of the thoracic aorta starting at the level of the tracheal bifurcation. Mean carotid lumen area was measured at 10 consecutive locations starting one slice below the level of the carotid bifurcation. Vessel wall calcifications were identified on the contrast enhanced CT scans by Hounsfield units ranging from 400 to 2000. Measurements were obtained in every vascular segment separately. Agatston scores for the carotid arteries, thoracic aorta, abdominal aorta, aorta and iliac arteries as well as the total Agatston score for all territories were used for further analysis [15]. Pericardial fat represents a composite of epicardial and paracardial fat and was defined as all voxels between the aortic root and the diaphragm with  $-30$  to  $-200$  Hounsfield units (Fig. 2) [14, 16, 17]. Both Agatston Score and pericardial fat volume parameters were assessed using the volume analysis tool of the cardiac workstation (Leonardo, Siemens AG, Healthcare Sector, Erlangen, Germany).

## Endpoints

Endpoints for the assessment of atherosclerosis progression included the annualized decrease in carotid and aortic lumen areas, annualized increase in carotid, aortic, iliac and total Agatston score as well as annualized increase in carotid, aortic, iliac and mean TBR values as calculated from the measurements obtained at baseline and follow-up  $^{18}\text{F}$ -FDG PET/CT.

## Statistical analysis

Categorical variables are presented as absolute and relative frequencies. Continuous variables are presented as mean and standard deviation. All changes (both absolute and percentages) are presented as annualized rates. Normal distribution of the data was assessed by histogram analysis and visual inspection. The one-sample *t* test was used for the comparison of annual change to zero. For between-group comparison unpaired Student *t* test was used. For the assessment of metric variables univariate regression analysis was performed. Predictors of atherosclerosis progression were assessed using multiple linear regression analysis with traditional risk factors (smoking, diabetes, hypertension, hypercholesterolemia, BMI and family history of CVD) and  $^{18}\text{F}$ -FDG PET/CT data (TBR, calcified wall volume and pericardial fat volume) included in the model. Furthermore patients were stratified and analyzed according to categories with low cardiovascular risk (no traditional risk factors), intermediate risk (1–2 risk factors) and high risk (3–6 risk factors). A *p* value of  $<0.05$  was chosen to indicate statistical significance. Statistical analysis was performed using SPSS for Windows, Version 19.0 (IBM, Chicago, IL, USA).

## Results

### Patient population

Baseline characteristics of the patients are reported in Table 1. We identified 163 patients with a contrast enhanced  $^{18}\text{F}$ -FDG PET/CT scan and a follow-up scan 9–24 months later between 2011 and 2012. Thirty-one patients received ongoing radiation therapy, in 21 patients the  $^{18}\text{F}$ -FDG PET/CT scan was performed due to suspected vasculitis or inflammation of unknown origin and 17 patients received steroid medication. Thus 94 patients with baseline and follow-up contrast-enhanced  $^{18}\text{F}$ -FDG PET/CT were included in the analysis. The mean (median) follow-up time was  $14.5 \pm 3.5$  months (14.0 months); range 9.0–24.0 months. The study population consisted mainly of female patients (64.9 %) with a mean age of 62.5 years. The indication for  $^{18}\text{F}$ -FDG PET/CT was cancer staging or suspected cancer in all patients. Patient suffered predominantly from colon/rectal cancer (20.2 %), cervical/ovarian cancer (20.2 %) or breast cancer (19.1 %). The study population included few diabetics (8.5 %) and many smokers (44.7 %). The prevalence of hypertension was 30.9 % and a positive family history of cardiovascular disease was present in 43.6 %. Although 36.2 % all patients had known hypercholesterolemia only 8.5 % received statin medication. Few patients had a history of coronary artery disease (9.6 %), previous myocardial

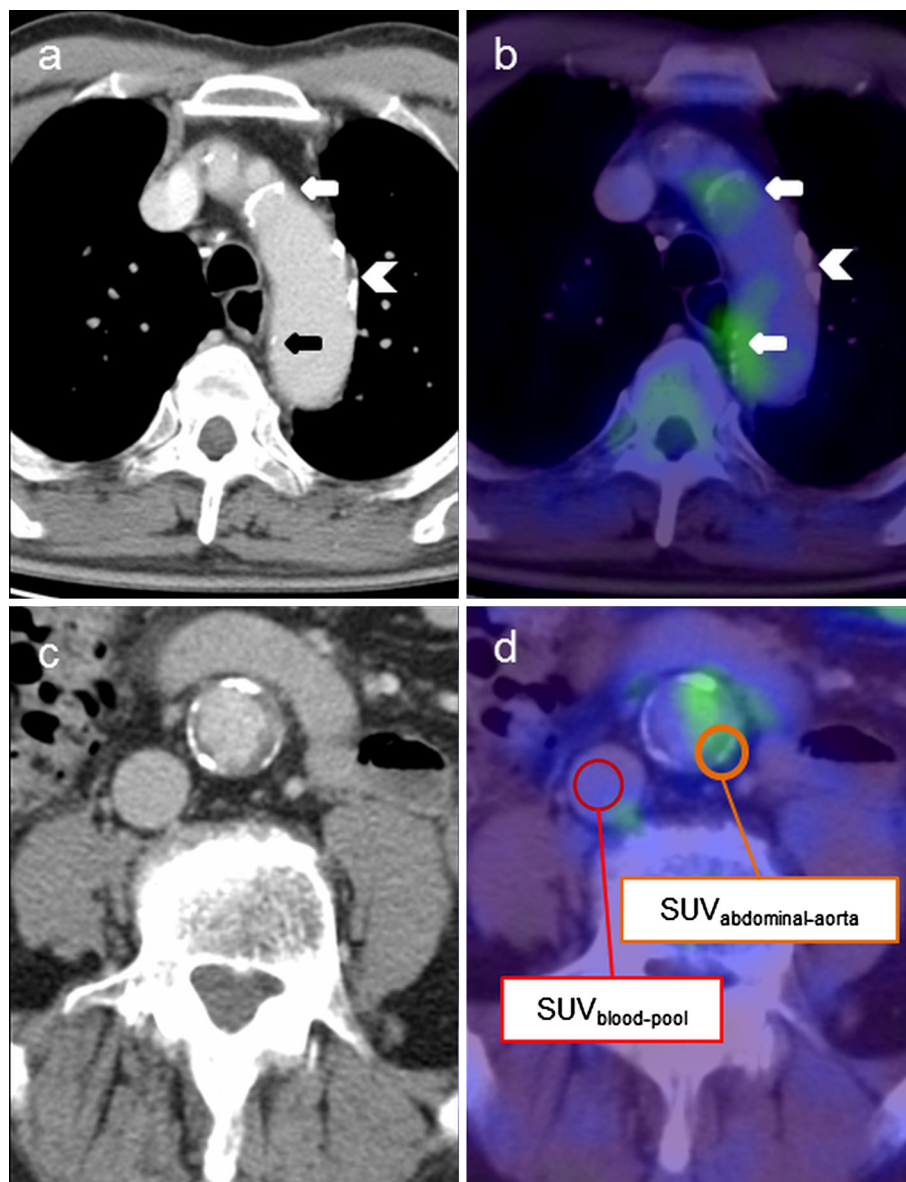


**Fig. 1**  $^{18}\text{F}$ -FDG PET/CT images of an inflamed, calcified atherosclerotic lesion. **a** and **b** show different calcified lesions in the aortic arch with (*arrows*) and without increased  $^{18}\text{F}$ -FDG-uptake (*chevrons*). Vessel wall calcifications were identified on the contrast enhanced CT scans by Hounsfield units ranging from 400 to 2000. To measure standard uptake values (SUV), circular regions of interest (ROIs) were placed over the carotid and iliac vessels to fully cover the arterial wall. In larger vessels, ROIs with a diameter of 1 cm were slid

along the circumference of the arterial wall to locate and measure the maximal SUV of the segment. **c** and **d** show cross-sections of the abdominal aorta and illustrate measurements of SUV in the blood-pool (*red circle*) and vessel wall (*orange circle*) that were used for calculations of target to background ratios (TBR) according to the following formula:  $\text{TBR}_{\text{abdominal-aorta}} = \text{SUV}_{\text{abdominal-aorta}} / \text{SUV}_{\text{blood-pool}}$

infarction (3.2 %) or transient ischemic attacks (3.2. %). At baseline or during follow-up 40.4 % of all patients received chemotherapy.

#### Baseline $^{18}\text{F}$ -FDG PET/CT data

Overall 564 vessel segments of 94 patients were assessed at baseline. Mean TBR for all vessel segments was  $1.44 \pm 0.18$  (range 1.08–1.88). High TBR values were observed in the

abdominal aorta and thoracic aorta [ $1.61 \pm 0.27$  (range 1.16–2.76) and  $1.58 \pm 0.23$  (range 1.17–2.35), respectively] while lower TBR values were measured in the carotid and iliac arteries [ $1.26 \pm 0.20$  (range 0.73–1.68) and  $1.35 \pm 0.23$  (range 0.95–2.10)]. Average Agatston score was  $89.7 \pm 276.5$  in the carotid arteries,  $520.0 \pm 1223.2$  in the thoracic aorta,  $1629.0 \pm 2823.1$  in the abdominal aorta and  $822.9 \pm 1316.3$  in the iliac arteries. Mean aortic and carotid lumen area were  $497.7 \pm 99.4 \text{ mm}^2$  (range

**Fig. 2** Measurement of pericardial fat. Pericardial fat was defined as a composite of epicardial and paracardial fat and measured as the combined volume of all mediastinal voxels between the aortic root and the diaphragm with  $-30$  to  $-200$  Hounsfield units. **a** shows a axial slice right above the diaphragm, **b** the result of the semiautomatic segmentation of pericardial fat (yellow area)

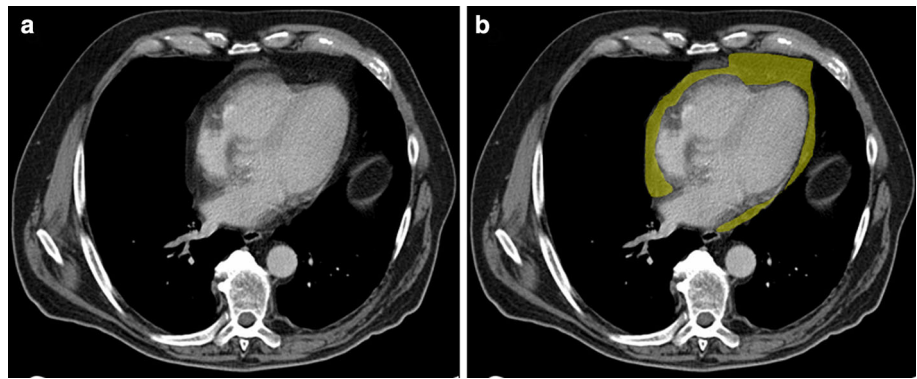


**Table 1** Baseline characteristics of study population

Parameter	Population (n = 94)
Mean age (years)	62.5 ± 8.7 (49.0, 81.0)
Men (n)	33 (35.1 %)
Body mass index	25.3 ± 4.3 (17.0, 36.7)
Mean follow-up time (months)	14.6 ± 3.5 (9.0, 24.0)
Cardiovascular risk factors (n)	
Hypercholesterolemia	34 (36.2 %)
Hypertension	29 (30.9 %)
Smoker	42 (44.7 %)
Diabetes mellitus	8 (8.5 %)
Family history of cardiovascular disease	41 (43.6 %)
Medical history	
Previous myocardial infarction	3 (3.2 %)
Previous transient ischemic attack	3 (3.2 %)
Coronary artery disease	9 (9.6 %)
Current statin medication	8 (8.5 %)
Ongoing chemotherapy	38 (40.4 %)
Cancer entities/indication for FDG PET/CT	
Head and neck	5 (5.3 %)
Lung	7 (7.4 %)
Oesophagus and stomach	2 (2.1 %)
Liver and biliary system	3 (3.2 %)
Pancreas	2 (2.1 %)
Colon and rectum	19 (20.2 %)
Kidney and urinary tract	3 (3.2 %)
Penis	5 (5.3 %)
Cervix and ovaries	19 (20.2 %)
Breast	18 (19.1 %)
Lymphoma	4 (4.3 %)
Chordoma	1 (1.1 %)
Cancer of unknown primary	5 (5.3 %)
No tumor	1 (1.1 %)

Values are mean ± standard deviation followed by range or number followed by percentage

318.3–787.1 mm<sup>2</sup>) and 54.0 ± 17.7 mm<sup>2</sup> (range 25.7–106.6 mm<sup>2</sup>), respectively. Average pericardial fat volume was 130.7 ± 65.6 cm<sup>3</sup> (range 27.4–373.3 cm<sup>3</sup>).

### Progression of <sup>18</sup>F-FDG PET/CT parameters

Average time between baseline and follow-up <sup>18</sup>F-FDG PET/CT was 14.6 ± 3.6 months (range 9.0–24.0 months). In the carotid arteries TBR values were significantly lower at follow-up with an annualized difference of  $-3.9$  % ( $p = 0.006$ ). There were trends towards lower values at follow-up for all vascular territories but these were not significant. When annualized TBR differences were compared among carotid arteries, aorta and iliac arteries no significant difference was observed (all  $p \geq 0.069$ ).

We observed a significant increase in annualized total Agatston score of 15.4 % ( $469.9 \pm 931.4$ ;  $p < 0.0001$ ). Calcifications advanced in all vascular territories (all  $p \leq 0.04$ ) but most pronounced in the thoracic and abdominal aorta with an annualized difference of 23.4 and 16.3 % ( $p < 0.0001$ ) as illustrated in Fig. 3. Over the follow-up period carotid artery and aortic lumen showed a significant reduction of  $-10.5$  and  $-1.7$  % (all  $p \leq 0.005$ ), respectively. Pericardial fat increased significantly with an annualized difference of 3.1 % ( $p = 0.026$ ). An overview of <sup>18</sup>F-FDG PET/CT derived parameters at baseline and follow-up is provided in Table 2.

### Predictors of disease progression

#### Univariate analysis

Patients with hypertension had significant more increase in overall calcified wall volume than patients without hypertension ( $969.27 \pm 1482.62$  vs.  $247.14 \pm 368.21$ ;  $p = 0.0001$ ). This difference was mainly driven by increased calcifications in the thoracic aorta ( $282.41 \pm 650.49$  vs.  $42.27 \pm 106.13$ ;  $p = 0.005$ ) and iliac arteries ( $196.19 \pm 450.38$  vs.  $-0.39 \pm 405.84$ ;  $p = 0.04$ ). Reduction of carotid lumen area was more pronounced in subjects with hypercholesterolemia ( $-2.66 \pm 8.01$  vs.  $7.70 \pm 8.91$ ;  $p = 0.008$ ). In unifactorial linear regression analysis BMI significantly predicted aortic lumen reduction ( $R^2 = 0.05$ ;

**Fig. 3** Progression of calcified atherosclerotic plaque. **a** shows a axial cross-section of the abdominal aorta at baseline with no detectable calcifications. After a follow-up of 12.5 months **b** this patient developed calcific plaque at the corresponding area (*arrow*)

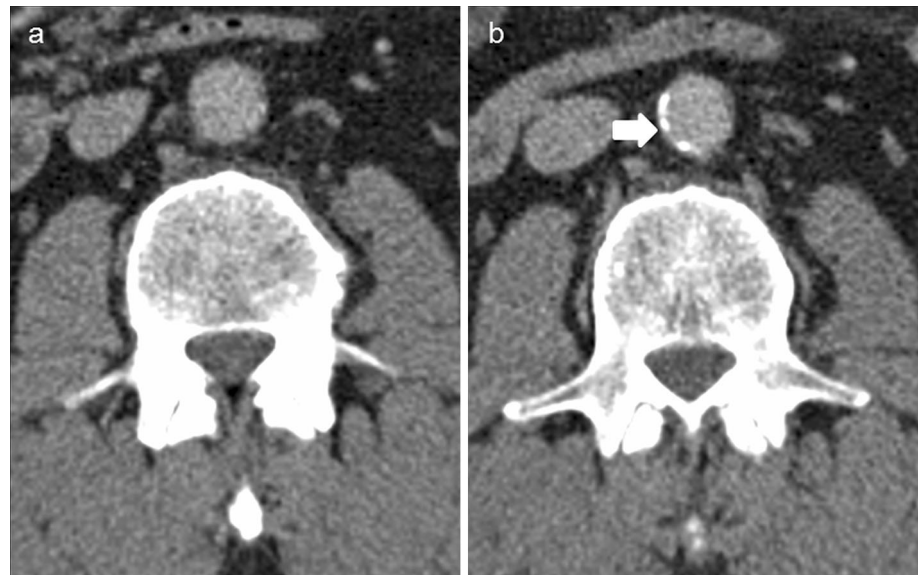


**Table 2**  $^{18}\text{F}$ -FDG PET/CT parameters at baseline and follow-up

Parameter	Baseline	Follow-up	<i>p</i> value	Absolute difference	Relative difference	Annualized absolute difference	Annualized relative difference
<b>TBR</b>							
Mean	1.45 ± 0.18	1.42 ± 0.19	0.18	-0.03 ± 0.17	-2.07	-0.02 ± 0.15	-1.71
Carotid arteries	1.26 ± 0.20	1.19 ± 0.20	0.006	-0.06 ± 0.21	-4.76	-0.05 ± 0.19	-3.92
Thoracic aorta	1.58 ± 0.23	1.55 ± 0.21	0.25	-0.03 ± 0.21	-1.90	-0.02 ± 0.19	-1.57
Adominal aorta	1.61 ± 0.27	1.61 ± 0.24	0.98	-0.00 ± 0.26	0.00	-0.00 ± 0.23	0.00
Aorta	1.59 ± 0.22	1.57 ± 0.20	0.35	-0.02 ± 0.20	-1.26	-0.01 ± 0.18	-1.04
Iliac arteries	1.35 ± 0.23	1.34 ± 0.24	0.70	-0.01 ± 0.25	-0.74	-0.00 ± 0.22	-0.61
<b>Agatston score</b>							
Sum	3061.48 ± 5030.75	3632.77 ± 6010.07	<0.0001	571.29 ± 1159.76	18.66	469.92 ± 931.43	15.37
Carotid arteries	89.68 ± 276.54	100.50 ± 281.24	0.031	10.82 ± 47.91	12.07	9.42 ± 42.31	9.95
Thoracic aorta	519.95 ± 1223.24	667.59 ± 1580.24	0.003	147.64 ± 471.67	28.40	116.36 ± 384.17	23.41
Adominal aorta	1629.00 ± 2823.07	1952.01 ± 3431.56	<0.0001	321.01 ± 776.64	19.71	283.89 ± 711.39	16.25
Aorta	2148.95 ± 3818.33	2619.60 ± 4711.88	<0.0001	470.65 ± 1099.18	21.90	400.24 ± 936.38	18.06
Iliac arteries	822.86 ± 1316.34	912.67 ± 1435.81	0.045	89.82 ± 428.80	10.92	60.26 ± 427.49	9.00
<b>Lumen (mm<sup>2</sup>)</b>							
Carotid arteries	54.01 ± 17.74	46.94 ± 18.28	<0.0001	-7.08 ± 10.24	-12.64	-5.87 ± 8.89	-10.46
Aorta	497.71 ± 99.42	488.38 ± 101.76	0.005	-9.33 ± 31.24	-1.83	-8.68 ± 26.15	-1.72
Pericardial fat (cm <sup>3</sup> )	130.74 ± 65.56	135.04 ± 69.28	0.026	4.30 ± 18.38	3.43	3.99 ± 17.38	3.05

TBR Target to background ratio

$p = 0.03$ ). Other analyzed parameters were not significant and are shown in Online Resource 1 and 2.

#### Multivariate analysis

In a multivariate linear regression analysis of traditional risk factors (smoking, diabetes, hypertension, hypercholesterolemia, BMI and family history of CVD) and

$^{18}\text{F}$ -FDG PET/CT data (TBR, calcified wall volume and pericardial fat volume) hypertension was the only independent predictor of total calcified wall volume progression ( $R^2 = 0.12$ ,  $p = 0.028$ ). When vascular territories were analyzed separately, hypertension predicted progression of calcifications in the thoracic aorta, aorta and iliac arteries ( $p \leq 0.039$ ). In the thoracic aorta a positive family history of CVD contributed to the model. Smoking

**Table 3** Predictors of atherosclerotic disease progression derived from multiple linear regression analysis

Dependent variable	Predictors in the model	B (95 %CI)	R <sup>2</sup>	p value
Calcified plaque progression				
Sum	Hypertension	723.34 (332.74–1113.93)	0.13	0.028
Thoracic aorta	Hypertension	263.06 (99.80–426.31)	0.13	0.002
	Family history of CVD	168.96 (16.63–321.28)		0.03
Aorta	Hypertension	511.43 (104.29–918.56)	0.06	0.014
Iliac arteries	Hypertension	198.07 (10.40–385.75)	0.05	0.039
TBR progression				
Mean	Smoking	0.09 (0.03–0.15)	0.08	0.006
Lumen reduction				
Carotid arteries	Hypercholesterolemia	−5.07 (−1.38–8.77)	0.08	0.008
Aorta	BMI	−1.99 (−0.76–3.22)	0.14	0.002
	TBR Mean	−42.40 (−71.94–12.86)		0.005

TBR target to background, BMI body mass index, CVD cardiovascular disease

significantly predicted progression of mean TBR ( $R^2 = 0.08$ ,  $p = 0.006$ ) but not TBR values in the separate vascular territories. Carotid lumen reduction was predicted by hypercholesterolemia ( $R^2 = 0.08$ ,  $p = 0.008$ ) while aortic lumen reduction was associated with BMI and mean TBR ( $R^2 = 0.14$ ,  $p \leq 0.005$ ). A summary of the different models is shown in Table 3.

*Analysis of risk categories*

We observed a trend to higher calcified wall volume in patients with more risk factors at both baseline and follow-up in all analyzed vascular territories (Fig. 4). These differences were significant in the abdominal aorta and aorta when low risk and moderate risk patients were compared (all  $p \leq 0.01$ ), in the iliac arteries when moderate risk and high risk patients were compared ( $p \leq 0.02$ ) and in the abdominal aorta, aorta and iliac arteries when low risk and high risk patients were compared (all  $p \leq 0.004$ ). Furthermore, vascular territories also experienced a significant different progression in calcified wall volume between baseline and follow-up depending on risk category (Fig. 5). The annualized difference in calcified wall volume in the abdominal aorta and aorta were significantly higher in the moderate and high risk group when compared to the low risk group ( $312.80 \pm 805.91$  and  $319.14 \pm 563.16$  vs.  $27.05 \pm 72.78$ ;  $p = 0.008$  and  $0.03$  for abdominal aorta;  $450.52 \pm 1085.02$  and  $405.37 \pm 627.08$  vs.  $77.27 \pm 173.26$ ;  $p = 0.01$  and  $p = 0.03$  for aorta, respectively). We did not observe a significant difference in the annualized difference of calcified plaque volume in any vascular territory between the moderate and high risk group ( $p \geq 0.15$ , Fig. 5). Furthermore we detected a smaller aortic lumen in the high risk population compared to the low risk population at both baseline ( $436.37 \pm 74.43$  vs.  $530.10 \pm 96.92$  mm<sup>2</sup>;  $p = 0.007$ ) and follow-up ( $411.45 \pm 84.01$  vs.  $527.04 \pm 106.05$  mm<sup>2</sup>;

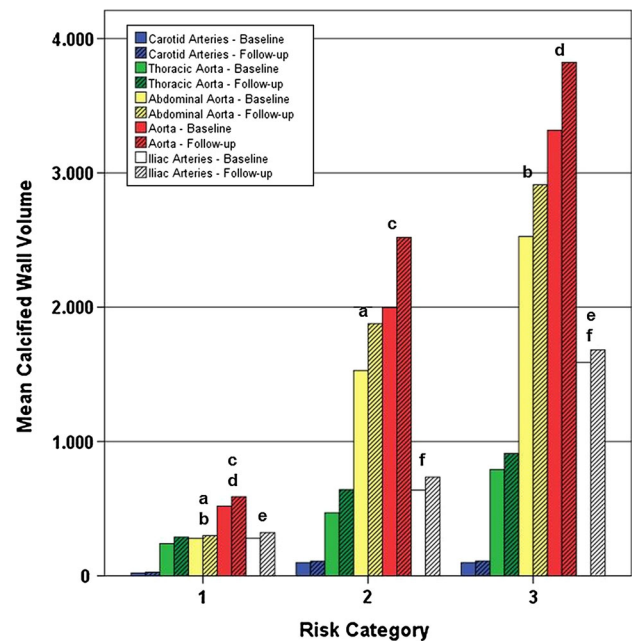


**Fig. 4** Calcified plaque volumes in different vascular territories at baseline and follow-up stratified by cardiovascular risk category. Patients were stratified as category 1 with low risk for cardiovascular events (no traditional risk factors), category 2 with intermediate risk (1–2 risk factors) or category 3 with high risk (3–6 risk factors). Risk factors included smoking, diabetes, hypertension, hypercholesterolemia, body mass index and family history of cardiovascular disease. There was a trend towards higher calcified plaque volume with increasing number of risk factors. This trend was significant in the abdominal aorta when category 1 was compared to category 2 (a) and category 3 (b). The same was true for the aorta (c and d). In the iliac arteries there was a significant difference when category 3 was compared to category 1 (e) and category 2 (f)

$p = 0.003$ ), annualized change in aortic lumen was not significantly different for both groups ( $p = 0.06$ ). There was no difference in TBR and carotid lumen among risk categories.

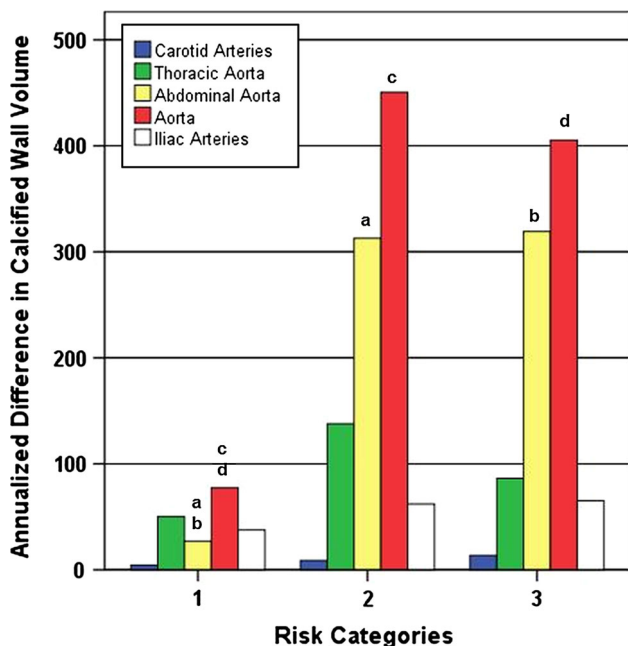


**Fig. 5** Annualized difference in calcified wall volume in different vascular beds stratified by cardiovascular risk category. Patients were stratified as category 1 with low risk for cardiovascular events (no traditional risk factors), category 2 with intermediate risk (1–2 risk factors) or category 3 with high risk (3–6 risk factors). Risk factors included smoking, diabetes, hypertension, hypercholesterolemia, body mass index and family history of cardiovascular disease. There was a trend towards increased progression of calcified plaque volume in all territories. This trend reached statistical significance in the abdominal aorta when category 1 was compared to categories 2 (a) and 3 (b). The same was true for the aorta (c and d)

## Discussion

This study provides data on the natural history and influencing factors of atherosclerosis disease progression in multiple vascular beds as derived by  $^{18}\text{F}$ -FDG PET/CT including calcified plaque burden carotid and aortic lumen as well as vessel wall inflammation.

Over a mean follow-up period of 15 months we observed a significant increase in calcified wall volume by 15.4 % and reduction in aortic and carotid lumen area by 1.7 % and 10.5 %, respectively, while there was a trend towards lower TBR values in most vascular territories.

We identified several factors that were associated with accelerated disease progression. More specifically, hypertension and family history of CVD predicted progression of atherosclerotic calcifications whereas smoking predicted progression of vascular inflammation. Carotid lumen reduction was associated with hypercholesterolemia and aortic lumen reduction was predicted by BMI and mean TBR, suggesting that vascular inflammation was associated with an accelerated progression of atherosclerosis in the aorta. Furthermore patients with a higher number of

traditional cardiovascular risk factors had a higher calcified plaque burden at baseline and follow-up as well as increased progression of calcified wall volume in the abdominal aorta and aorta.

These results are in line with earlier studies in coronary arteries evaluating the effect of various cardiovascular risk factors on the prevalence, extent and progression on calcified plaque burden. Coronary calcifications were linked to hypertension, hypercholesterolemia, diabetes and smoking [18–21].

However, data on the influence of these risk factors on other vascular beds was limited and restricted to certain patient populations. In patients with a history of ischemic stroke or transient ischemic attack, newly detectable calcifications and annual calcification growth in carotid arteries have been found to be associated with age, hypertension and smoking [22]. Carotid atherosclerosis and disease progression has been associated with a variety of cardiovascular risk factors including hypercholesterolemia in both younger and older cohorts [23–25]. Aortic wall thickening has been used to evaluate the progression of aortic atherosclerosis [26, 27]. However, we were unable to identify reports that study the natural history of aortic calcifications.

Ectopic fat deposits like pericardial fat, abdominal visceral fat, intramuscular or intrahepatic fat release various bioactive substances that influence insulin resistance, glucose and lipid metabolism and inflammation, which all contribute to cardiovascular risk [28]. Pericardial fat releases cytokines like leptin, resistin, tumor necrosis factor- $\alpha$ , interleukin-6, visfatin, and chemerin and has been associated with progression of coronary atherosclerosis as detected by coronary artery calcium scoring [28–30]. We did not observe any effect of the amount of paracardial fat on atherosclerotic disease extent or progression in other vascular territories, which is compatible with a locally limited paracrine and proinflammatory activity of pericardial fat [31].

Interestingly we did not observe an association between vessel wall inflammation and progression of arterial wall calcifications. Atherosclerotic plaque formation is a sequential process with inflammation as the predominant mechanism in early plaque stages. During this inflammation  $^{18}\text{F}$ -FDG peaks and erosion of the fibrous cap may lead to thromboembolic events [9, 32]. The inflammatory process also initiates calcium metabolism with formation of early calcium deposits. While this process might be visualized by hydroxyapatite-specific  $^{18}\text{F}$ -sodiumfluoride PET imaging, early calcium deposits might not be visualized by CT imaging until their density reaches a certain threshold. Mineralization process may exceed inflammatory activity within atherosclerotic lesions with decreasing  $^{18}\text{F}$ -FDG uptake but ongoing increase in calcified wall volume [32,



33]. Given the relative large amount of arterial wall calcification it might be speculated that most atherosclerotic lesions in this patient population were not at the state of maximum inflammation at the time of baseline imaging or that active inflammation is not the driving force of ongoing calcification in later plaque stages. Other markers of atherosclerosis progression like reduction in lumen area might be more suitable to assess the impact on inflammation. This hypothesis is underlined by the observed significant reduction in aortic lumen area which was predicted by baseline TBR. Other promising markers to assess atherosclerotic disease progression/regression would be wall volume and volume of soft plaque. However the imaging protocol in this study was not optimized for vascular imaging and therefore these parameters could not be obtained with satisfying accuracy.

We observed smaller TBR values in smaller vessels. This might in part be explained by partial volume effects. In addition, the arterial wall thickness is substantially smaller in smaller vessels which might also contribute to smaller TBR values. Last but not least the plaque burden might differ across vessel wall territories and might also contribute to the observed differences.

The results of the current and previous studies underline the potential of  $^{18}\text{F}$ -FDG PET/CT for the assessment of cardiovascular disease. However,  $^{18}\text{F}$ -FDG PET/CT also suffers from various drawbacks including radiation exposure, high direct costs for the examination and high indirect costs associated with the evaluation of potential incidental finding that are derived during  $^{18}\text{F}$ -FDG PET/CT due to the whole body approach. While these drawbacks might be acceptable in research studies, they currently hamper the widespread use of  $^{18}\text{F}$ -FDG PET/CT in the clinical setting.

## Limitations

Our cohort consisted of cancer patients that underwent  $^{18}\text{F}$ -FDG PET/CT imaging during routine staging. In this population other effects such as paraneoplastic phenomena and chemotherapy might also play an important role in atherosclerosis initiation and development and may attenuate the effects of other risk factors. Since cancer type, stage and treatment varied substantially in our patient cohort and the study was not sufficiently powered to detect differences within treatment and disease groups these factors were not included within the model. However, the substantial radiation exposure of repeated full body  $^{18}\text{F}$ -FDG PET/CT scans [34] and strict national guidelines for reduction of radiation exposure necessitated a cohort in which  $^{18}\text{F}$ -FDG PET/CT is indicated for cancer evaluation.

Precise measurements of cardiovascular risk factors such as blood cholesterol levels and blood pressure were

not available which prevented calculation and analysis of the Framingham or comparable risk scores.

The average follow-up period of approximately 15 months was limited which might at least in part explain why vessel wall inflammation did not change significantly during the time course of this study. However, other  $^{18}\text{F}$ -FDG PET/CT studies in even smaller cohorts have demonstrated that statin therapy induced changes of FDG-uptake can be observed in less than four months [35], suggesting that any change which might have occurred during the follow-up period of about 15 months was rather small and clinically not significant.

In order to accommodate for differences of the time between baseline and follow-up scan we used annualized parameters to provide estimates independent of the exact observation time. However this approach assumes a linear progression of atherosclerosis over time, which may be problematic given the different stages within the complicated disease process.

Important vascular territories such as the coronary, intracranial or calf arteries were not accessible in this study since our imaging protocol was optimized for staging of cancer patients and not for full body vascular imaging.

Images were acquired approximately 60 min after injection of  $^{18}\text{F}$ -FDG, as required in our cancer protocol for detection of tumors, although longer circulation times have been recommended for optimized detection of plaque inflammation [36].

In general the correlation between atherosclerotic disease progression and  $^{18}\text{F}$ -FDG PET/CT derived parameters as well as conventional risk factors were weak. This might in part be attributed to the retrospective design of the study and the limitations mentioned above. One might speculate that correlations would have been stronger in a prospective study with an optimized cardiovascular  $^{18}\text{F}$ -FDG PET/CT protocol, a hypothesis which needs to be tested in future studies.

## Conclusion

In this study we were able to identify several factors, such as hypertension, vessel wall inflammation, hypercholesterolemia and BMI which were associated with accelerated atherosclerotic disease progression in distinct vascular beds. In addition we were able to provide data on the natural history of atherosclerosis disease progression outside the coronary tree as assessed by  $^{18}\text{F}$ -FDG PET/CT. Further  $^{18}\text{F}$ -FDG PET/CT studies in non-oncological patients are necessary to better elucidate the role of risk factors on plaque progression and more importantly to identify factors that are associated with the occurrence of cardio- or cerebrovascular events.

**Conflict of interest** The authors declare that they have no conflict of interest.

**Ethical standard** All procedures performed in studies involving human participants were in accordance with the ethical standards of the institutional and/or national research committee and with the 1964 Helsinki declaration and its later amendments or comparable ethical standards.

**Informed consent** Informed consent was obtained from all individual participants included in the study.

## References

1. Stary HC, Chandler AB, Dinsmore RE et al (1995) A definition of advanced types of atherosclerotic lesions and a histological classification of atherosclerosis. A report from the Committee on Vascular Lesions of the Council on Arteriosclerosis, American Heart Association. *Circulation* 92:1355–1374
2. Naghavi M, Libby P, Falk E et al (2003) From vulnerable plaque to vulnerable patient: a call for new definitions and risk assessment strategies: Part I. *Circulation* 108:1664–1672
3. Rosamond W, Flegal K, Furie K et al (2008) Heart disease and stroke statistics–2008 update: a report from the American Heart Association Statistics Committee and Stroke Statistics Subcommittee. *Circulation* 117:e25–146
4. den Ruijter HM, Peters SA, Groenewegen KA et al (2013) Common carotid intima-media thickness does not add to Framingham risk score in individuals with diabetes mellitus: the USE-IMT initiative. *Diabetologia* 56:1494–1502
5. Saam T, Hetterich H, Hoffmann V et al (2013) Meta-analysis and systematic review of the predictive value of carotid plaque hemorrhage on cerebrovascular events by magnetic resonance imaging. *J Am Coll Cardiol* 62:1081–1091
6. Bamberg F, Sommer WH, Hoffmann V et al (2011) Meta-analysis and systematic review of the long-term predictive value of assessment of coronary atherosclerosis by contrast-enhanced coronary computed tomography angiography. *J Am Coll Cardiol* 57:2426–2436
7. Chow BJ, Wells GA, Chen L et al (2010) Prognostic value of 64-slice cardiac computed tomography severity of coronary artery disease, coronary atherosclerosis, and left ventricular ejection fraction. *J Am Coll Cardiol* 55:1017–1028
8. Otaki Y, Rajani R, Cheng VY et al (2011) The relationship between epicardial fat volume and incident coronary artery calcium. *J Cardiovasc Comput Tomogr* 5:310–316
9. Rominger A, Saam T, Wolpers S et al (2009) 18F-FDG PET/CT identifies patients at risk for future vascular events in an otherwise asymptomatic cohort with neoplastic disease. *J Nucl Med* 50:1611–1620
10. Rudd JH, Warburton EA, Fryer TD et al (2002) Imaging atherosclerotic plaque inflammation with [18F]-fluorodeoxyglucose positron emission tomography. *Circulation* 105:2708–2711
11. Tawakol A, Migrino RQ, Bashian GG et al (2006) In vivo 18F-fluorodeoxyglucose positron emission tomography imaging provides a noninvasive measure of carotid plaque inflammation in patients. *J Am Coll Cardiol* 48:1818–1824
12. Strobl FF, Rominger A, Wolpers S et al (2013) Impact of cardiovascular risk factors on vessel wall inflammation and calcified plaque burden differs across vascular beds: a PET-CT study. *Int J Cardiovasc Imaging* 29:1899–1908
13. Falk E, Sillesen H, Muntendam P, Fuster V (2011) The high-risk plaque initiative: primary prevention of atherothrombotic events in the asymptomatic population. *Curr Atheroscler Rep* 13:359–366
14. Saam T, Rominger A, Wolpers S et al (2010) Association of inflammation of the left anterior descending coronary artery with cardiovascular risk factors, plaque burden and pericardial fat volume: a PET/CT study. *Eur J Nucl Med Mol Imaging* 37:1203–1212
15. Agatston AS, Janowitz WR, Hildner FJ, Zusmer NR, Viamonte M Jr, Detrano R (1990) Quantification of coronary artery calcium using ultrafast computed tomography. *J Am Coll Cardiol* 15:827–832
16. Greif M, Leber AW, Saam T et al (2012) Determination of pericardial adipose tissue increases the prognostic accuracy of coronary artery calcification for future cardiovascular events. *Cardiology* 121:220–227
17. Greif M, Becker A, von Ziegler F et al (2009) Pericardial adipose tissue determined by dual source CT is a risk factor for coronary atherosclerosis. *Arterioscler Thromb Vasc Biol* 29:781–786
18. Kronmal RA, McClelland RL, Detrano R et al (2007) Risk factors for the progression of coronary artery calcification in asymptomatic subjects: results from the Multi-Ethnic Study of Atherosclerosis (MESA). *Circulation* 115:2722–2730
19. Cassidy-Bushrow AE, Bielak LF, Sheedy PF II et al (2007) Coronary artery calcification progression is heritable. *Circulation* 116:25–31
20. Tomizawa N, Nojo T, Inoh S, Nakamura S (2015) Difference of coronary artery disease severity, extent and plaque characteristics between patients with hypertension, diabetes mellitus or dyslipidemia. *Int J Cardiovasc Imaging* 31:205–212
21. Hadamitzky M, Meyer T, Hein F et al (2012) Prognostic value of coronary computed tomographic angiography in patients with arterial hypertension. *Int J Cardiovasc Imaging* 28:641–650
22. van Gils MJ, Bodde MC, Cremers LG, Dippel DW, van der Lugt A (2013) Determinants of calcification growth in atherosclerotic carotid arteries; a serial multi-detector CT angiography study. *Atherosclerosis* 227:95–99
23. Rozie S, de Weert TT, de Monye C et al (2009) Atherosclerotic plaque volume and composition in symptomatic carotid arteries assessed with multidetector CT angiography; relationship with severity of stenosis and cardiovascular risk factors. *Eur Radiol* 19:2294–2301
24. Juonala M, Magnussen CG, Venn A et al (2010) Influence of age on associations between childhood risk factors and carotid intima-media thickness in adulthood: the Cardiovascular Risk in Young Finns Study, the Childhood Determinants of Adult Health Study, the Bogalusa Heart Study, and the Muscatine Study for the International Childhood Cardiovascular Cohort (i3C) Consortium. *Circulation* 122:2514–2520
25. Chambless LE, Folsom AR, Davis V et al (2002) Risk factors for progression of common carotid atherosclerosis: the Atherosclerosis Risk in Communities Study, 1987–1998. *Am J Epidemiol* 155:38–47
26. Arai Y, Hirose N, Yamamura K et al (2002) Long-term effect of lipid-lowering therapy on atherosclerosis of abdominal aorta in patients with hypercholesterolemia: noninvasive evaluation by a new image analysis program. *Angiology* 53:57–68
27. Takasu J, Masuda Y, Watanabe S et al (1994) Progression and regression of atherosclerotic findings in the descending thoracic aorta detected by enhanced computed tomography. *Atherosclerosis* 110:175–184
28. Lim S, Meigs JB (2014) Links between ectopic fat and vascular disease in humans. *Arterioscler Thromb Vasc Biol* 34:1820–1826
29. Yerramasu A, Dey D, Venuraju S et al (2012) Increased volume of epicardial fat is an independent risk factor for accelerated progression of sub-clinical coronary atherosclerosis. *Atherosclerosis* 220:223–230
30. Nakanishi R, Rajani R, Cheng VY et al (2011) Increase in epicardial fat volume is associated with greater coronary artery calcification progression in subjects at intermediate risk by

- coronary calcium score: a serial study using non-contrast cardiac CT. *Atherosclerosis* 218:363–368
31. Sacks HS, Fain JN (2007) Human epicardial adipose tissue: a review. *Am Heart J* 153:907–917
  32. Cocker MS, Mc Ardle B, Spence JD et al (2012) Imaging atherosclerosis with hybrid [(18)F]fluorodeoxyglucose positron emission tomography/computed tomography imaging: what Leonardo da Vinci could not see. *J Nucl Cardiol* 19:1211–1225
  33. Koenig W, Khuseyinova N (2007) Biomarkers of atherosclerotic plaque instability and rupture. *Arterioscler Thromb Vasc Biol* 27:15–26
  34. Brix G, Lechel U, Glatting G et al (2005) Radiation exposure of patients undergoing whole-body dual-modality 18F-FDG PET/CT examinations. *J Nucl Med* 46:608–613
  35. Tahara N, Kai H, Ishibashi M et al (2006) Simvastatin attenuates plaque inflammation: evaluation by fluorodeoxyglucose positron emission tomography. *J Am Coll Cardiol* 48:1825–1831
  36. Rudd JH, Myers KS, Bansilal S et al (2008) Atherosclerosis inflammation imaging with 18F-FDG PET: carotid, iliac, and femoral uptake reproducibility, quantification methods, and recommendations. *J Nucl Med* 49:871–878